European Conference on Computational Fluid Dynamics
ECCOMAS CFD 2006
P. Wesseling, E. Oñate and J. Périaux (Eds)

NUMERICAL CONTROL OF NORMAL VELOCITY BY NORMAL STRESS FOR INTERACTION BETWEEN AN INCOMPRESSIBLE FLUID AND AN ELASTIC CURVED ARCH

C.M. Murea[*] and C. Vázquez[†]

[*]Laboratoire de Mathématiques, Informatique et Applications,
Université de Haute-Alsace, France
e-mail: cornel.murea@uha.fr
web page: http://www.edp.uha.fr/murea/
[†]Departamento de Matemáticas, Facultad de Informática,
Universidade da Coruña, Spain
e-mail: carlosv@udc.es

Key words: Fluid-structure interaction, Stokes equations, curved arch, optimal control, finite elements

Abstract. *We study the fluid-structure coupled problem between an incompressible fluid and an elastic curved arch. The fluid flow is modeled by 2-D steady Stokes equations with normal velocity boundary condition on the curved interface and the arch verifies a particular 1-D case of the thin shell theory of Koiter. We present an optimal control formulation for this fluid-arch interaction. More precisely, the control is the normal force acting on the interface and the observation is the normal velocity of the fluid on the interface. Numerical results arising from modelling blood flow in arteries are presented.*

1 PRESENTATION OF THE PROBLEM

Let us consider a fluid which fills a two-dimensional domain Ω_u^F, the boundary of which is composed by the inflow section Σ_1, the rigid boundary Σ_2, the outflow section Σ_3 and the interface between the fluid and the structureΓ_u. The boundary Γ_u depends on the displacement $\mathbf{u}$ of the elastic arch. Moreover, we denote by $\mathbf{n} = (n_1, n_2)^T$ the unit outward normal vector and by $\boldsymbol{\tau} = (-n_2, n_1)^T$ the unit tangential vector to the boundary of the fluid domain (see Figure 1).

The fluid flow is modeled by the steady Stokes equations and the arch verifies a particular case of the thin shell theory of Koiter. Thus, for a given pressure on the inflow and outflow sections, the coupled problem is to find the displacement $\mathbf{u}$ of the arch, the velocity $\mathbf{v}$ and the pressure p of the fluid.

This kind of fluid-structure interaction arises in some processes of the cardiovascular system, for example, blood-heart interaction[1,2], blood flow in large arteries[3,4,5], arteries

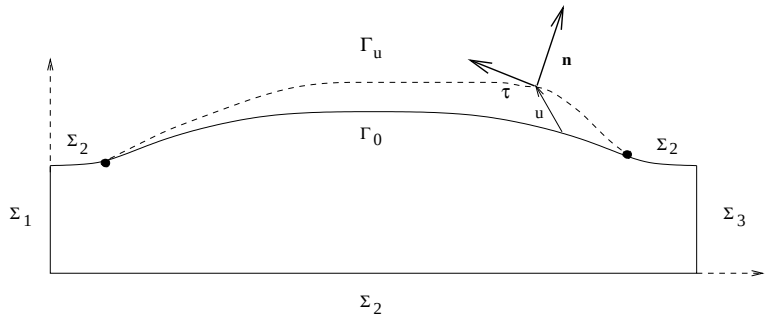

Figure 1: Geometrical model and notations for a fluid-structure interaction with curved interface

with aneurysm, air flow in artificial lungs[6], or in the car industries, for example fluid flow in a shock absorber[7].

2 WEAK FORMULATION OF THE ARCH PROBLEM

In this section, we first adapt from Bernadou-Lucatel[8] the usual notations in thin shell theory.

Let $L > 0$ and $\phi^1, \phi^2 : [0, L] \to \mathbb{R}$ so that the parametric description of the undeformed arch is given by:

$$\Gamma_0 = \left\{(x_1, x_2) \in \mathbb{R}^2;\ x_1 = \phi^1(\xi),\ x_2 = \phi^2(\xi),\ \xi \in [0, L]\right\}.$$

That is, the boundary Γ_0 is the image of the map $\boldsymbol{\phi} = (\phi^1, \phi^2) : [0, L] \to \mathbb{R}^2$. We denote by $'$ the derivative with respect ξ. Then, the covariant basis $(\mathbf{a_1}, \mathbf{a_3})$ is given by

$$\mathbf{a_1} = \left(\left(\phi^1\right)', \left(\phi^2\right)'\right)^T, \quad \mathbf{a_3} = \frac{1}{\sqrt{a}}\left(\left(\phi^2\right)', -\left(\phi^1\right)'\right)^T$$

and the associated contravariant basis $(\mathbf{a^1}, \mathbf{a^3})$ is

$$\mathbf{a^1} = \frac{1}{\sqrt{a}}\mathbf{a_1}, \quad \mathbf{a^3} = \mathbf{a_3}$$

where $a = \left(\left(\phi^1\right)'\right)^2 + \left(\left(\phi^2\right)'\right)^2$. So, we have $\|\mathbf{a^1}\| = \|\mathbf{a^3}\| = \|\mathbf{a_3}\| = 1$, where $\|\cdot\|$ is the Euclidean norm in $\mathbb{R}^2$. Notice thay in general $\|\mathbf{a_1}\| \neq 1$. Next, we associate to any displacement field $\boldsymbol{\psi} = \psi_1\mathbf{a^1} + \psi_3\mathbf{a^3}$ the 1-D plane strain (γ) and change of curvature tensors (ρ)

$$\gamma_1^1(\boldsymbol{\psi}) = \frac{1}{\sqrt{a}}\left(\left(\frac{\psi_1}{\sqrt{a}}\right)' + \frac{\sqrt{a}}{R}\psi_3\right), \quad \rho_1^1(\boldsymbol{\psi}) = \frac{1}{\sqrt{a}}\left(\frac{1}{\sqrt{a}}\left(\psi_3' - \frac{1}{R}\psi_1\right)\right)'$$

where

$$\frac{1}{R} = \frac{\left(\phi^1\right)'\left(\phi^2\right)'' - \left(\phi^1\right)''\left(\phi^2\right)'}{a^{3/2}}.$$

Now, we introduce the admissible displacement space, U, given by

$$\mathbf{U} = \left\{ \boldsymbol{\psi} = (\psi_1, \psi_3) \in H_0^1(]0, L[) \times H_0^2(]0, L[) \right\}.$$

Thus, assuming an elastic, homogeneous and isotropic arch, we define the bilinear form $a_S : U \times U \to \mathbb{R}$ by

$$a_S(\mathbf{u}, \boldsymbol{\psi}) = \frac{Ee}{1-\nu^2} \int_0^L \left(\gamma_1^1(\boldsymbol{u})\, \gamma_1^1(\boldsymbol{\psi}) + \frac{e^2}{12} \rho_1^1(\boldsymbol{u})\, \rho_1^1(\boldsymbol{\psi}) \right) \sqrt{a}\, d\xi$$

where $e > 0$, $E > 0$ and $0 < \nu < 1/2$ denote the thickness, the Young's modulus and the Poisson's ratio of the arch, respectively.

Weak formulation of the arch displacement problem

For given $\mathbf{f}^S = \left(f^{S,1}, f^{S,3}\right)$ and $\boldsymbol{\lambda} = (\lambda^1, \lambda^3)$ this formulation is posed as follows:

Find $\mathbf{u} = (u_1, u_3) \in U$, such that:

$$a_S(\mathbf{u}, \boldsymbol{\psi}) = \int_0^L \left(\lambda^1 \psi_1 + \lambda^3 \psi_3 \right) \sqrt{a}\, d\xi + \int_0^L \left(f^{S,1} \psi_1 + f^{S,3} \psi_3 \right) \sqrt{a}\, d\xi,\ \forall \psi \in U. \quad (1)$$

Proposition 1 *Let $\mathbf{f}^S = \left(f^{S,1}, f^{S,3}\right)$ and $\boldsymbol{\lambda} = (\lambda^1, \lambda^3)$ in $L^2(]0, L[) \times L^2(]0, L[)$. Then, the problem (1) has an unique solution.*

A standard reference for the existence results in shell theory is Ciarlet[9].

The physical meaning of $\mathbf{f}^S$ is that of an external volume force applied to the elastic arch (for example, the gravity forces). In a fluid-structure interaction problem, $\boldsymbol{\lambda}$ is associated to the surface forces from the fluid acting on the structure.

Thus, the parametric description of the deformed arch is

$$\Gamma_u = \left\{ (x_1, x_2) \in \mathbb{R}^2; (x_1, x_2)^T = \boldsymbol{\phi}(\xi) + u_1(\xi)\mathbf{a^1}(\xi) + u_3(\xi)\mathbf{a^3}(\xi), \xi \in [0, L] \right\}.$$

3 MIXED HYBRID FORMULATION OF THE FLUID PROBLEM

Strong form of the fluid equations

For given μ, $\mathbf{f}^F$, P_{in} and σ^F, this problem is posed as follows:

Find $\mathbf{v} : \Omega_u^F \to \mathbb{R}^2$ and $p : \Omega_u^F \to \mathbb{R}$ such that:

$$\begin{aligned}
-\mu \Delta \mathbf{v} + \nabla p &= \mathbf{f}^F, \quad \text{in } \Omega_u^F && (2)\\
\nabla \cdot \mathbf{v} &= 0, \quad \text{in } \Omega_u^F && (3)\\
\mathbf{v} \times \mathbf{n} &= 0, \quad \text{on } \Sigma_1 && (4)\\
\mathbf{n} \cdot \left(\sigma^F \mathbf{n}\right) &= -P_{in}, \quad \text{on } \Sigma_1 && (5)\\
\mathbf{v} &= 0, \quad \text{on } \Sigma_2 && (6)\\
\mathbf{v} \times \mathbf{n} &= 0, \quad \text{on } \Sigma_3 && (7)\\
\mathbf{n} \cdot \left(\sigma^F \mathbf{n}\right) &= -P_{out}, \quad \text{on } \Sigma_3 && (8)\\
\mathbf{v} \times \mathbf{n} &= 0, \quad \text{on } \Gamma_u && (9)\\
\mathbf{n} \cdot \left(\sigma^F \mathbf{n}\right) &= -\lambda^3 \circ \left(\boldsymbol{\phi} + u_1 \mathbf{a^1} + u_3 \mathbf{a^3}\right)^{-1}, \quad \text{on } \Gamma_u && (10)
\end{aligned}$$

where

- $\mu > 0$ is the viscosity of the fluid,
- $\mathbf{f}^F = (f_1^F, f_2^F)$ are the applied volume forces, in general the gravity forces,
- $P_{in} : \Sigma_1 \to \mathbb{R}$ and $P_{out} : \Sigma_3 \to \mathbb{R}$ are prescribed normal boundary forces,
- $\sigma^F = -p\, I + \mu \left(\nabla \mathbf{v} + \nabla \mathbf{v}^T\right)$ is the stress tensor of the fluid.

In two-dimensions, we have $\mathbf{v} \times \mathbf{n} = v_1 n_2 - v_2 n_1$.

Remark 1 *Condition (10) is a consequence of the action and reaction principle concerning the normal stress on the interface. Since* $\mathbf{n} \cdot \left(\sigma^F \mathbf{n}\right)$ *is defined on* Γ_u*, while* λ^3 *is defined on* $[0, L]$*, we have to use in (10) the inverse of the map* $\boldsymbol{\phi} + u_1 \mathbf{a^1} + u_3 \mathbf{a^3}$*. We will come back to this topic in Section 4.*

Weak formulation of the fluid problem

We introduce the following Hilbert spaces:

$$\begin{aligned} \mathbf{W} &= \left\{ \mathbf{w} = (w_1, w_2) \in \left(H^1\left(\Omega_u^F\right)\right)^2;\ \mathbf{w} = 0 \text{ on } \Sigma_2,\ v_2 = 0 \text{ on } \Sigma_1 \cup \Sigma_3 \right\}, \\ Q &= L^2\left(\Omega_u^F\right), \\ Z &= H^{1/2}\left(\Gamma_u\right). \end{aligned}$$

Since Σ_1 and Σ_3 are vertical boundaries, the conditions (4) and (7) are equivalent with $w_2 = 0$ on $\Sigma_1 \cup \Sigma_3$.

We denote by $\epsilon(\mathbf{v}) = (\epsilon_{ij}(\mathbf{v}))_{1 \le i,j \le 2}$, the strain rate tensor, where $\epsilon_{ij}(\mathbf{v}) = \frac{1}{2}\left(\frac{\partial v_i}{\partial x_j} + \frac{\partial v_j}{\partial x_i}\right)$. Next, let us consider the maps $a_F : \mathbf{W} \times \mathbf{W} \to \mathbb{R}$, $b_F : \mathbf{W} \times Q \to \mathbb{R}$ and $c_F : \mathbf{W} \times Z \to \mathbb{R}$, defined by

$$\begin{aligned} a_F(\mathbf{v}, \mathbf{w}) &= 2\mu \sum_{i,j=1}^{2} \int_{\Omega_u^F} \epsilon_{ij}(\mathbf{v}) \epsilon_{ij}(\mathbf{w})\, d\mathbf{x} \\ b_F(\mathbf{w}, q) &= -\int_{\Omega_u^F} (\nabla \cdot \mathbf{w})\, q\, d\mathbf{x} \\ c_F(\mathbf{w}, \zeta) &= -\int_{\Gamma_u} (\mathbf{w} \cdot \boldsymbol{\tau})\, \zeta\, d\gamma \\ \ell_F(\mathbf{w}) &= \int_{\Omega_u^F} \mathbf{f}^F \cdot \mathbf{w}\, d\mathbf{x} - \int_{\Gamma_u} (\mathbf{w} \cdot \mathbf{n})\, \lambda^3 \circ \left(\boldsymbol{\phi} + u_1 \mathbf{a^1} + u_3 \mathbf{a^3}\right)^{-1} d\gamma \\ &\quad - \int_{\Sigma_1} (\mathbf{w} \cdot \mathbf{n})\, P_{in}\, d\gamma - \int_{\Sigma_3} (\mathbf{w} \cdot \mathbf{n})\, P_{out}\, d\gamma \end{aligned}$$

The weak form of Problem (2)–(10) is posed as follows:
Find $\mathbf{v} \in \mathbf{W}$, $p \in Q$ and $\eta \in Z$, such that

$$\begin{aligned} a_F(\mathbf{v},\mathbf{w}) + b_F(\mathbf{w},p) + c_F(\mathbf{w},\eta) &= \ell_F(\mathbf{w}),\ \forall \mathbf{w} \in \mathbf{W} \quad (11)\\ b_F(\mathbf{v},q) &= 0,\ \forall q \in Q \quad (12)\\ c_F(\mathbf{v},\zeta) &= 0,\ \forall \zeta \in Z \quad (13)\end{aligned}$$

The physical meaning of η is that of the tangential stress on the interface, i.e. $\eta = \boldsymbol{\tau} \cdot \sigma^F \mathbf{n}$, while the mathematical meaning is that of a Lagrange multiplier associated to the constraint $\mathbf{v} \cdot \boldsymbol{\tau} = 0$ on the interface.

The system (11)–(13) is a mixed-hybrid like problem[10]. The bilinear form a_F is continuous and elliptic[11] only if the map from $\mathbf{W}$ to $Q \times Z$

$$\mathbf{w} \mapsto (-\nabla \cdot \mathbf{w}, -\mathbf{w} \cdot \boldsymbol{\tau}|_{\Gamma_u}) \quad (14)$$

is onto.

The problem (11)–(13) is similar to the mixed-hybrid system[12,13], but in this papers the condition $\mathbf{v} \cdot \mathbf{n} = 0$ is treated by a Lagrange multiplier.

Strong and weak treatment of the condition $\mathbf{v} \cdot \boldsymbol{\tau} = 0$ is analyzed in Pironneau[14].

4 COUPLED FLUID-ARCH PROBLEM

The fluid and the arch problems are coupled via two boundary conditions: continuity of velocity and stress on the interface.

Since the velocity of the arch is zero in the steady case, we search a solution of the coupled problem such that $\mathbf{v} = 0$ on the interface. From condition (9), we have $\mathbf{v} \cdot \boldsymbol{\tau} = 0$ on Γ_u. So, in order to obtain the continuity of the velocity at the interface, it remains to find a fluid velocity such that $\mathbf{v} \cdot \mathbf{n} = 0$ on Γ_u.

The surface forces acting on the arch in a point $\boldsymbol{\phi}(\xi)$ of Γ_0 are given by

$$\lambda^1 \mathbf{a_1} + \lambda^3 \mathbf{a_3},$$

while the surface forces acting on the fluid in the point $\boldsymbol{\phi}(\xi) + u_1(\xi)\mathbf{a^1}(\xi) + u_3(\xi)\mathbf{a^3}(\xi)$ of Γ_u are given by

$$\sigma^F \mathbf{n} = \left(\boldsymbol{\tau} \cdot \left(\sigma^F \mathbf{n}\right)\right) \boldsymbol{\tau} + \left(\mathbf{n} \cdot \left(\sigma^F \mathbf{n}\right)\right) \mathbf{n}.$$

In the case of small displacements, we assume that

$$\frac{1}{\sqrt{a}} \mathbf{a_1} = \mathbf{a^1} \approx \boldsymbol{\tau}, \quad \mathbf{a_3} = \mathbf{a^3} \approx \mathbf{n}.$$

So, according with the action and reaction principle, it follows that

$$-\lambda^1 \sqrt{a} \approx \boldsymbol{\tau} \cdot \left(\sigma^F \mathbf{n}\right) = \eta$$

and

$$-\lambda^3 \approx \mathbf{n} \cdot \left(\sigma^F \mathbf{n}\right).$$

The last condition is handled by (10) in the fluid problem.

For a given $\boldsymbol{\lambda}$, we obtain the displacement $\mathbf{u}$ by solving the arch problem (1). Then, from the fluid problem (11)–(13), we get the velocity $\mathbf{v}$, the pressure p of the fluid and the tangential stress on the interface η.

Thus, the fluid-arch interaction problem is to find $\boldsymbol{\lambda}$ such that

$$\mathbf{v} \cdot \mathbf{n} = 0, \text{ on } \Gamma_u \tag{15}$$

$$-\lambda^1 \sqrt{a} = \eta \circ \left(\boldsymbol{\phi} + u_1 \mathbf{a^1} + u_3 \mathbf{a^3}\right), \text{ on } [0, L]. \tag{16}$$

Notice that equation (16) represents the continuity of the tangential stress on the interface.

We recall that the tangential velocity of the fluid vanishes (see equation (7)) and the continuity of the normal stress on the interface is treated by (10).

In the following, we assume that the arch displacement only depends on λ^3. This is true in the cardiovascular system, where the blood pressure is more important than the viscous part of the stress tensor, so the normal component of the stress,

$$\mathbf{n} \cdot \left(\sigma^F \mathbf{n}\right) = -p + \mu\, \mathbf{n} \cdot \left(\nabla \mathbf{v} + \nabla \mathbf{v}^T\right) \mathbf{n},$$

is very large compared to the tangential component

$$\boldsymbol{\tau} \cdot \left(\sigma^F \mathbf{n}\right) = \mu\, \boldsymbol{\tau} \cdot \left(\nabla \mathbf{v} + \nabla \mathbf{v}^T\right) \mathbf{n}.$$

Then, Problem (1) can be written as:

Find $\mathbf{u} = (u_1, u_3) \in U$, such that:

$$a_S(\mathbf{u}, \boldsymbol{\psi}) = \int_0^L \lambda^3 \psi_3 \sqrt{a}\, d\xi + \int_0^L \left(f^{S,1}\psi_1 + f^{S,3}\psi_3\right) \sqrt{a}\, d\xi,\ \forall \psi \in U. \tag{17}$$

The tangential deformation of the arch is not null in general, even though the stress on the interface is normal.

The solution $(\mathbf{v},\ p,\ \eta)$ of the fluid problem (11)-(13) does not depend on λ^1, so if we set:

$$\lambda^1 = -\frac{1}{\sqrt{a}} \eta \circ \left(\boldsymbol{\phi} + u_1 \mathbf{a^1} + u_3 \mathbf{a^3}\right),$$

then the condition (16) holds.

Now, the coupled fluid-arch problem can be posed as:

Find λ^3 (the normal stress on the interface) such that $\mathbf{v} \cdot \mathbf{n}|_{\Gamma_u} = 0$.

We transform this exact controllability problem into the following optimal control one:

$$\inf\ \frac{1}{2} \int_{\Gamma_u} (\mathbf{v} \cdot \mathbf{n})^2\ d\gamma, \tag{18}$$

subject to :

$$- \quad \lambda^3 \in L^2\left(]0, L[\right) \tag{19}$$

$$- \quad u \text{ solution of the arch problem (17)} \tag{20}$$

$$- \quad (\mathbf{v},\ p,\ \eta) \text{ solution of the fluid problem (11)} - \text{(13)} \tag{21}$$

This formulation generalizes the work in Murea-Vázquez[15] to the case of elastic curved interface.

5 NUMERICAL RESULTS

In this section we present some illustrative test examples concerning the blood flow in arteries.

Geometry data

For $L = 6\ cm$, the parametric description of the undeformed arch is given by

$$\Gamma_0 = \left\{(x_1, x_2) \in \mathbb{R}^2;\ x_1 = \xi,\ x_2 = -5 + \sqrt{45 - (\xi - 3)^2},\ \xi \in [0, L]\right\}.$$

The top boundary of the fluid domain (see Figure 1) is composed by the arch in the middle, the following fixed boundary at the left

$$\Sigma_2^l = \left\{x_1 = \xi,\ x_2 = 0.1\xi^3 + 0.4\xi^2 + 0.5\xi + 1,\ \xi \in [-1, 0]\right\}$$

and the following fixed boundary at the right

$$\Sigma_2^r = \left\{x_1 = \xi,\ x_2 = -0.1\xi^3 + 2.2\xi^2 - 16.1\xi + 40,\ \xi \in [6, 7]\right\}.$$

The bottom of the fluid domain is $\Sigma_2^d = \{(x, 0)/ - 1 \leq x \leq 7\}$, while the inflow boundary, Σ_1, and outflow one, Σ_3, are appropriate vertical segments of length $0.8cm$.

Physical parameters

In the arch problem, the thickness of the elastic wall is $e = 0.1\ cm$, the Young's modulus is taken to $E = 0.75 \cdot 10^6\ \frac{g}{cm \cdot s^2}$, the Poisson's ratio is $\nu = 0.49$ and the mass density is $\rho^S = 1.1\ \frac{g}{cm^3}$.

In the fluid problem, the blood viscosity was taken to be $\mu = 0.035\ \frac{g}{cm \cdot s}$. Moreover, the volume force is $\mathbf{f}^F = (0, 0)^T$ and the outflow pressure is $P_{out} = 0$.

Finite elements discretization

The normal displacement of the arch is approached by $\mathbb{P}_3$ Hermite finite elements, while the tangential displacement is approached by $\mathbb{P}_1$ finite elements on segments.

For the approximation of the fluid velocity and pressure we have employed the triangular $\mathbb{P}_1$+*bubble* and $\mathbb{P}_1$ finite elements, respectively. The tangential stress on the interface is approached by $\mathbb{P}_1$ finite elements on segments.

Notice that the arch and the fluid meshes do not necessarily match themselves and, in general, the fluid mesh is much finer than the structure mesh.

All the fluid meshes are obtained by moving a fixed mesh with a displacement which is the solution of a Laplace problem with Dirichlet boundary conditions. On the fixed boundaries, Σ_1, Σ_2 and Σ_3, the mesh displacement vanishes, while it is equal to the arch displacement on the interface Γ_u.

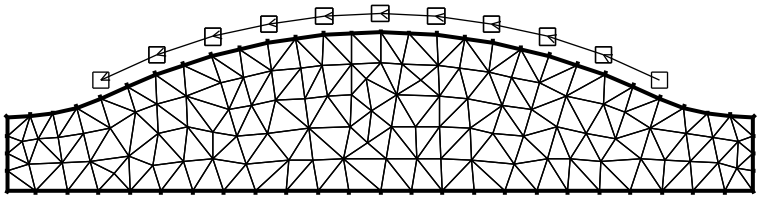

Figure 2: Typical fluid and arch meshes

Numerical solution of the optimal control problem

In order to solve numerically Problem (18)–(21), the Broyden, Fletcher, Goldforb, Shano (BFGS) method has been used, where the gradient of the cost function was approached by a first order finite differences method with the grid spacing 0.01.

Moreover, we have used the stopping criteria $|J| < \epsilon_1$ or $\|\nabla J\|_\infty < \epsilon_2$.

5.1 Control of normal velocity by normal stress on interface

In all the following numerical tests, the arch mesh has 10 segments (see Figure 2). Let $\{0 = \xi_0 < \xi_1 < \cdots < \xi_{10} = L\}$ be a uniform partition of the interval $[0, L]$. The normal stress on the interface λ^3 is approached by $\lambda_h^3 \in \mathcal{C}[0, L]$, $\lambda_h^3 \in \mathbb{P}_1$ on each segment $[\xi_i, \xi_{i+1}]$, $i = 0, \ldots, 9$.

In all the simulations, for solving the optimization problem, the initial used value is

$$\lambda_h^3(\xi_i) = P_{out} + (P_{in} - P_{out})\frac{10 - i}{10}, \quad i = 0, \ldots, 10.$$

We have used the stopping criteria $\|\nabla J\|_\infty < 0.05$.

Fluid mesh with 20 segments on the interface

In this test the fluid mesh has 226 triangles, 144 vertices and 20 segments on the elastic boundary. The solution of the optimal control problem verifies $\|\nabla J\|_\infty = 1.9 \cdot 10^{-2}$. The sequence of values of cost function produced by the BFGS method is shown in Table 1.

Iteration	J	Iteration	J
0	2547.091786	8	1.023813629
1	1211.782266	9	0.541353106
2	725.6283591	10	0.196142907
3	510.1113951	11	0.074620024
4	55.08303685	12	0.061075290
5	14.69322181	13	0.059283206
6	2.761055109	14	0.059257208
7	1.355973240		

Table 1: The BFGS iterations when fluid mesh has 20 segments on the interface

Fluid mesh with 50 segments on the interface

In this case, the fluid mesh has 1406 triangles, 779 vertices and 50 segments on the elastic boundary, the results being shown in Table 2. The last iteration value of the optimal control problem verifies $\|\nabla J\|_\infty = 1.0 \cdot 10^{-2}$.

Iteration	J	Iteration	J
0	2961.338390	7	8.851579284
1	2160.756802	8	2.369258721
2	1392.917188	9	1.271752295
3	879.6830449	10	0.382701032
4	206.9249346	11	0.179680309
5	28.11455274	12	0.124469558
6	18.81352198	13	0.123437472

Table 2: The BFGS iterations when fluid mesh has 50 segments on the interface

Fluid mesh with 80 segments on the interface

In this test, the fluid mesh has 3644 triangles, 1943 vertices and 80 segments on the elastic boundary, the associated results are shown in Table 3. The solution of the optimal control problem verifies $\|\nabla J\|_\infty = 3.3 \cdot 10^{-2}$.

Discussion of numerical results

Since the arch mesh has 10 segments and the normal stress on the interface is approached by the finite element $\mathbb{P}_1$, then the optimization problem obtained after the finite element approximation of (18)–(21) is of dimension 11.

Previous numerical results show that we can obtain very small normal velocity on 80 segments of the interface, using only 11 scalar controls.

Iteration	J	Iteration	J
0	3619.097215	6	29.86861359
1	1503.175625	7	13.36326171
2	258.7993032	8	10.33965940
3	91.91149097	9	0.753294422
4	61.75894998	10	0.095747979
5	42.29953564	11	0.092956444

Table 3: The BFGS iterations when fluid mesh has 80 segments on the interface

The optimal control problem (18)–(21) is a nonlinear least squares like system with zero residual. In our case, the residual function is the normal velocity on the interface. We try to find the normal stress on the interface such that the residual function vanishes.

Notice that the BFGS is an algorithm for general unconstrained optimization problems, that is not specially designed for the least squares problems. Despite of this, the BFGS method finds very small residual function in our application. A standard reference for nonlinear least squares problems is Dennis-Schnabel[16].

The optimal values of the cost function 0.05, 0.12, 0.09 obtained for the fluid meshes with 20, 50, 80 segments on the interface is not a decreasing sequence. One reason could be the fact that the BFGS method doesn't find the global minimum, but a local one. A second reason is the following: after the finite element discretization of the arch equations, it is possible that the optimal value of the cost function is not zero even for very fine fluid meshes.

5.2 Computed solutions for some inflow pressure

The interest in the following numerical simulation study lies in predicting the deformations of the arterial wall which are dependent on the fluid pressure at the inflow section.

In the simulations presented in this section the arch mesh has 10 segments. Moreover, all the fluid meshes have 516 triangles, 304 vertices and 30 segments on the elastic boundary Γ_u.

The tests correspond to the numerical solution of the fluid-structure problem for the following inflow pressures: $P_{in} = 50,\ 100,\ 200,\ 400\ dyn/cm^2$.

As stopping criteria in the BGFS algorithm we have chosen $|J| < 0.5$ or $\|\nabla J\|_\infty < 0.1$. The starting point for the BFGS method for $P_{in} = 100$ was the numerical solution obtained for $P_{in} = 50$ and so on.

P_{in}	initial J	final J	no. BFGS iterations
50	2928.63	0.23	9
100	356.86	0.26	13
200	1378.34	0.56	17
400	5257.25	2.08	20

Table 4: Results obtained by BFGS method for different inflow pressure

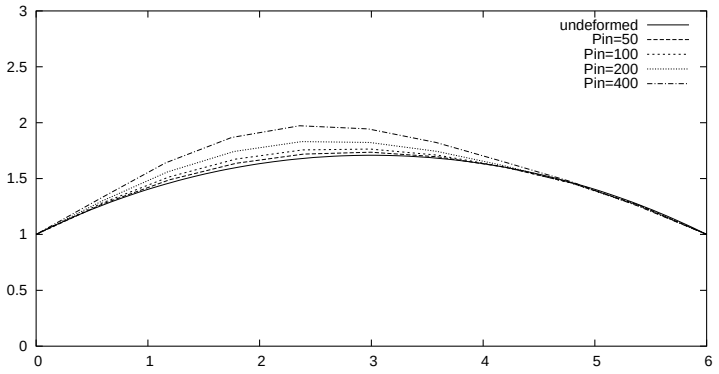

Figure 3: Deformations $[cm]$ of the boundary for different inflow pressures

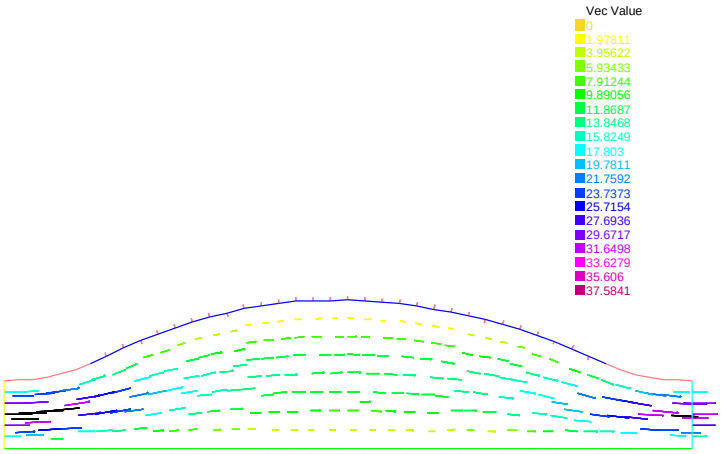

Figure 4: Fluid velocities $[cm/s]$ scaled by a factor 0.008 in the case $P_{in} = 50\ dyn/cm^2$

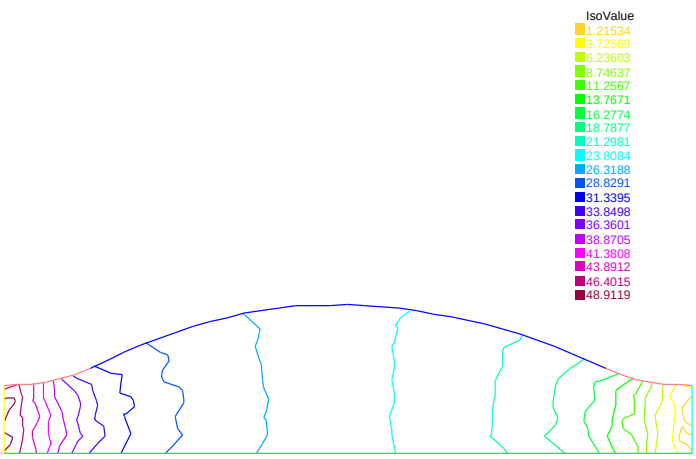

Figure 5: Fluid pressure $[dyn/cm^2]$ in the case $P_{in} = 50$

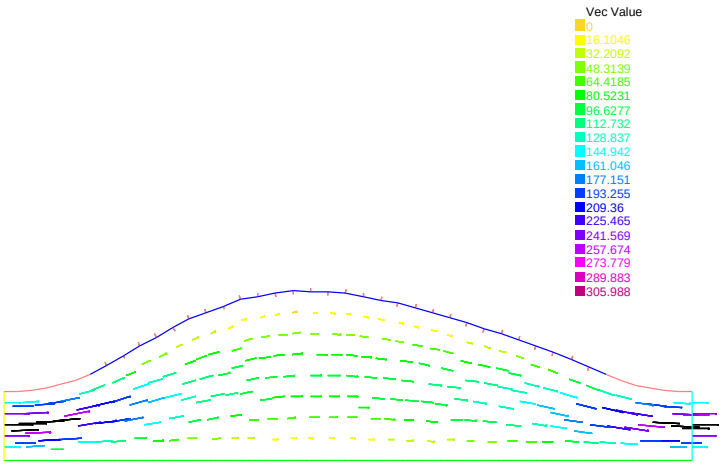

Figure 6: Fluid velocities $[cm/s]$ scaled by a factor 0.001 in the case $P_{in} = 400\ dyn/cm^2$

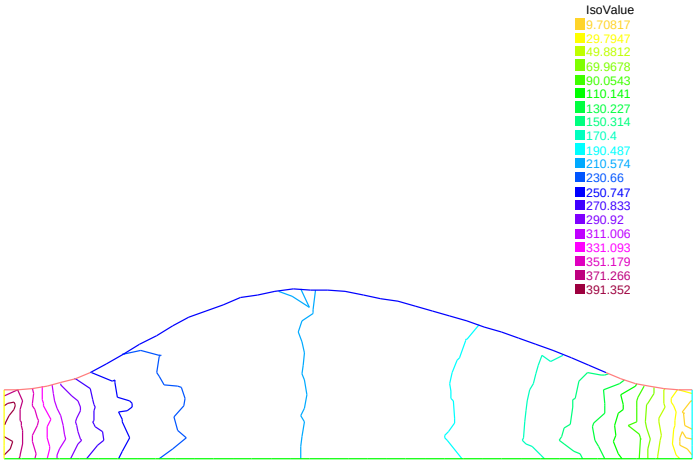

Figure 7: Fluid pressure $[dyn/cm^2]$ in the case $P_{in} = 400$

6 CONCLUSIONS

We have formulated a fluid-structure interaction as an optimal control problem. The control is the normal force acting on the interface and the observation is the normal velocity of the fluid on the interface.

The BFGS method finds numerically small residual function even for a reduced number of controls.

REFERENCES

[1] Y. Maday, B. Maury, P. Metier, Interaction de fluides potentiels avec une membrane élastique, in *ESAIM Proc.* **10** (1999), Soc. Math. Appl. Indust., Paris, pp. 23–33.

[2] F. N. van de Vosse, J. de Hart, C. H. G. A. van Oijen, D. Bessems, T. W. M. Gunther, A. Segal, B. J. B. M. Wolters, J. M. A. Stijnen, F. P. T. Baaijens, Finite-element-based computational methods for cardiovascular fluid-structure interaction. Mathematical modelling of the cardiovascular system. *J. Engrg. Math.* **47** (2003), no. 3-4, 335–368.

[3] A. Quarteroni, M. Tuveri, A. Veneziani, Computational vascular fluid dynamics: problems, models and methods. *Comput. Visual. Sci.* **2** (2000) 163–197.

[4] A. Quarteroni, L. Formaggia, Mathematical Modelling and Numerical Simulation of the Cardiovascular System. Chapter in *Modelling of Living Systems*, Ed. N. Ayache, Handbook of Numerical Analysis Series, vol. XII, Elsevier, Amsterdam, 2004.

[5] M.A. Fernández, J.-F. Gerbeau, C. Grandmont, A projection semi-implicit scheme for the coupling of an elastic structure with an incompressible fluid. To appear in *International Journal for Numerical Methods in Engineering* (2006)

[6] K.-J. Bathe, H. Zhang, Finite element developments for general fluid flows with structural interactions, *Int. J. Numer. Meth. Engng.* **60** (2004) 213–232.

[7] P. Le Tallec, J. Mouro, Fluid-structure interaction with large structural displacements, *Comput. Methods Appl. Mech. Engrg.* **190** (2001) (24-25), 3039–3067

[8] M. Bernadou, Y. Ducatel, Approximation of general arch problems by beam elements, Rapport de recherche INRIA no 120, Rocquencourt, 1982.

[9] Ph. Ciarlet, *Mathematical elasticity. Vol. III. Theory of shells.* Studies in Mathematics and its Applications, 29. North-Holland Publishing Co., Amsterdam, 2000.

[10] F. Brezzi, M. Fortin, *Mixed and Hybrid Finite Element Methods*, Springer Verlag, 1991.

[11] V. Girault, P.A. Raviart, *Finite Element Methods for Navier-Stokes Equations. Theory and Algorithms*, Springer Verlag, 1986.

[12] R. Verfurth, Finite element approximation of incompressible Navier-Stokes equations with slip boundary condition, *Numer. Math.*, **50** (1987) 697–721.

[13] R. Verfurth, Finite element approximation of incompressible Navier-Stokes equations with slip boundary condition II, *Numer. Math.*, **59** (1991) 615–636.

[14] O. Pironneau, Conditions aux limites sur la pression pour les équations de Stokes et Navier-Stokes, *C.R. Acad. Sc. Paris*, **303** (1986), Série I, No. 9, 403–406.

[15] C. Murea, C. Vazquez, Sensitivity and approximation of the coupled fluid-structure equations by virtual control method. *Appl. Math. Optim.*, **52** (2005), no. 2, 357–371.

[16] J.E. Dennis Jr., R.B. Schnabel, Numerical methods for unconstrained optimization and nonlinear equations. Classics in Applied Mathematics, 16. Society for Industrial and Applied Mathematics, Philadelphia, PA, 1996.